Proceedings of

2nd WORKSHOP on HTS Applications and New Materials

University of Twente, Enschede, The Netherlands
8, 9 and 10 May 1995

Edited by: Dave H.A. Blank

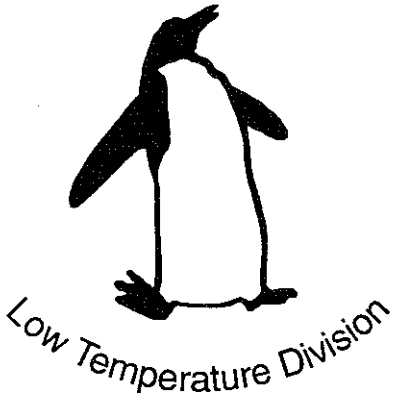

University of Twente
The Netherlands

Published by

Low Temperature Division
Department of Applied Physics
University of Twente
P.O.Box 217, 7500 AE Enschede
The Netherlands
Fax: xx-31-534891099
E-mail: D.H.A.Blank@tn.utwente.nl

Branches on the family tree: Superconductivity in epitaxial films of "first-in-line" descendants of the parent compound $SrCuO_2$

R. Feenstra, J. D. Budai, D. P. Norton, E. C. Jones, D. K. Christen, and T. Kawai[a]
Oak Ridge National Laboratory, P.O. Box 2008, Oak Ridge, Tennessee 37831
[a] *ISIR-Sanken, Osaka University, 8-1 Mihogaoka, Ibaraki, Osaka 567, Japan*

The defect-induced carrier doping in epitaxial films of the parent compound $SrCuO_2$ is reviewed. Two superconducting descendants were synthesized by expanding the role of natural defects in the parent $SrCuO_2$ films, namely, the Ruddlesheim-Popper phases $Sr_{n+1}Cu_nO_{2n+1}$ and a nonstoichiometric variant of the oxycarbonate $Sr_2CuO_2(CO_3)$. The synthesis and structures are described.

Introduction

Composed of CuO_2 sheets separated by layers of alkaline earth ions only, the "parent" or "infinite layer" compounds $ACuO_2$ (*A*: Ca-Sr-Ba) assume a pivotal position among the high temperature superconductor (HTS) copper oxides. The structure is isomorphic with the $Ca_{n-1}Cu_nO_{2n}$ perovskite-like cores of established HTS cuprates, such as the Bi-, Tl-, and Hg-based homologous series, and thus may be regarded the *invariant* $n\rightarrow\infty$ member of these series. The composition closest realizing this extrapolation is the original parent $Ca_{0.86}Sr_{0.14}CuO_2$, the only composition stable at ambient pressure [1]. The insulating and antiferromagnetic nature of this parent compound [2] clearly underscores the essential role of the various charge reservoir layers. On the other hand, bulk-like superconductivity has been observed for infinite layer compounds containing larger proportions of the alkaline earth metals Sr or Ba [3]. Analogous to the insulating parents of, say, the "214" and "123" type superconductors, $Ca_{0.86}Sr_{0.14}CuO_2$, therefore, also may be considered the insulating parent for these superconducting compositions, although the relation with the carrier doping defects is less straightforward. Continued research on these "infinite layer" superconductors has led to the synthesis of new homologous series of HTS cuprates, most notably the "$02(n-1)n$" series in the Sr(Ca)–Cu–O system [4] and the "$Cu–12(n-1)n$" series in the Ba–Ca–Cu–O system [5]. The charge reservoir layers in these compounds apparently are based on natural tendencies towards defect formation in the constituent $SrCuO_2$ and $BaCuO_2$ blocks. The identification of these tendencies greatly contributes to a better understanding of the underlying structural relations for the HTS cuprates and forms the basis of a systematic search for new compounds [6].

The research described in this work concerns the derivation of two superconducting "descendants" from epitaxial films of the intermediate endmember $SrCuO_2$. Contrary to high-pressure synthesized bulk ceramics of this composition [3], bulk-like superconductivity typically does not occur for the infinite layer films, although some tantalizing anomalies have been reported [7, 8]. (More recently, "infinite layer" films that exhibit reproducible superconducting properties have been synthesized in the form of superlattices containing (oxygen-defective) $BaCuO_2$ [9]). A starting point of the research, therefore, has been the identification of natural tendencies towards defect formation and carrier doping in the $SrCuO_2$ epitaxial films [10]. Some general trends of this defect-induced doping mechanism are reviewed below as a prelude to the superconducting descendants, schematically depicted in Fig. 1. The first of these, $SrCuO_2$ films containing artificially inserted SrO defects [11], is similar to the "$02(n-1)n$" Ruddlesheim-Popper phases synthesized in the bulk [4]. The critical role of charge neutrality constraints in the synthesis and post-growth oxidation of the epitaxial films will be discussed. The second superconducting descendant is a nonstoichiometric variant of the oxycarbonate $Sr_2CuO_2(CO_3)$ [12]. Recently, several reports have indicated that carbonate groups may readily substitute for Cu in HTS perovskite-like lattices

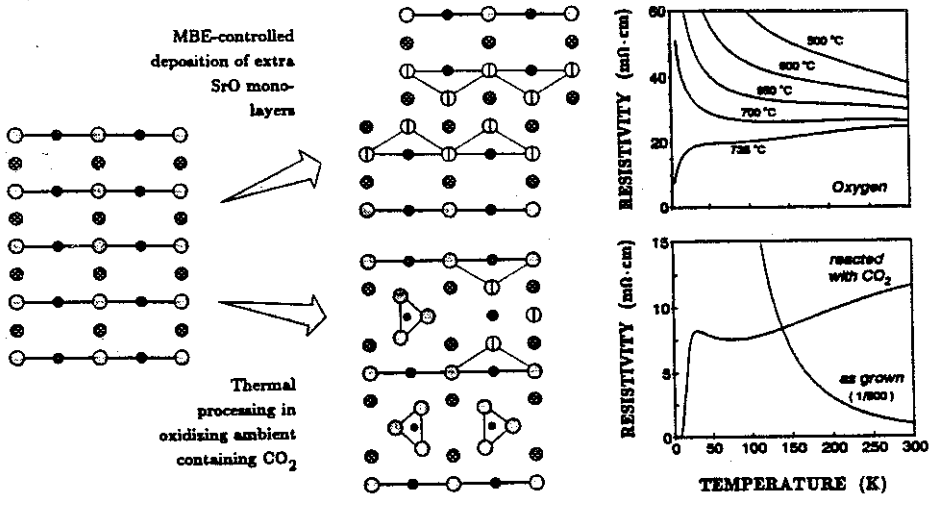

Fig. 1 Schematic representation of the introduction of charge reservoir layers in the $SrCuO_2$ infinite layer lattice. Oxygen sites expected to be partially occupied are indicated by open circles with vertical line. The onset of superconductivity is illustrated on the right.

and thus should be considered a naturally occurring defect [13]. An earlier report by Lindemer et al. [14] also indicates that, even in a widely investigated material such as $YBa_2Cu_3O_7$, carbon substitution levels less than 1% are difficult to achieve. To study the effect of carbon for the $SrCuO_2$ epitaxial films, as-grown films were annealed in oxidizing ambients containing small amounts of CO_2. These annealing studies led to the discovery of a conversion into the oxycarbonate structure, occurring at sufficiently high temperatures and CO_2 partial pressures [15]. Basic features of the oxycarbonate structure will be briefly described, as well as a model for the doping mechanism.

Defect formation and carrier doping in $SrCuO_2$ films

$Sr_xCuO_{2\pm\delta}$ films with various $x = Sr/Cu$ compositions were epitaxially grown on (100) $SrTiO_3$ substrates either by codeposition via single target pulsed-laser ablation (ORNL), or atomic layer stacking of Sr(O) and CuO_y monolayers using RHEED-controlled laser-MBE (Osaka). The system at ORNL uses a KrF excimer laser (248 nm). The deposition takes place in an oxygen ambient of which the pressure was varied between 2–200 mTorr [8, 16]. The system at Osaka University uses an ArF excimer laser (193 nm) and the deposition is performed in a low pressure of NO_2 oxidant (10^{-6}–10^{-4} mbar) to facilitate simultaneous operation of the RHEED [10, 17]. The target manipulation required for atomic layer stacking is computer-controlled. Typical substrate temperatures for either growth method ranged from 500°C to 550°C.

To study the nature of the majority charge carriers, reversible changes in the oxygen content were induced via low temperature anneals (350°C) at variable oxygen pressures. The anneals were performed in flowing mixtures of oxygen and argon at a total pressure of 1.0 atm [10]. Since oxygen attracts electrons (adds holes), hole-like and electron-like contributions lead to distinct dependencies of the resistivity on the oxygen pressure. Thus, low resistivities result for electron-doped films upon reduction of the oxygen content, while for hole-doped films the resistivity decreases upon oxidation. Typical effects from the Sr/Cu composition and deposition conditions for a series of co-deposited $Sr_xCuO_{2\pm\delta}$ films are summarized in Fig. 2. The following trends may be inferred: (i) The resistivity for films grown at low oxygen pressures decreases upon Sr-vacancy incorporation (for $x > 0.85$, films 1–3). Contrary to the expectation, however, and contrary

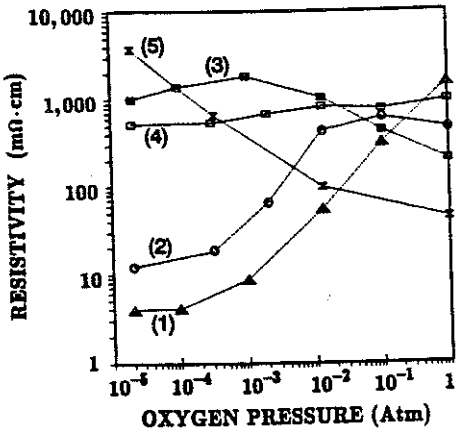

Fig. 2 Variation of the resistivity at 300 K with oxygen pressure during low temperature annealing (350°C) for codeposited $Sr_xCuO_{2\pm\delta}$ infinite layer films: (1) x = 0.85, (2) x = 1.0, (3) x = 1.2; (1)–(3): 550°C/2 mTorr; (4) x = 1.0 (550°C/200 mTorr); (5) x = 1.0 (500°C/200 mTorr).

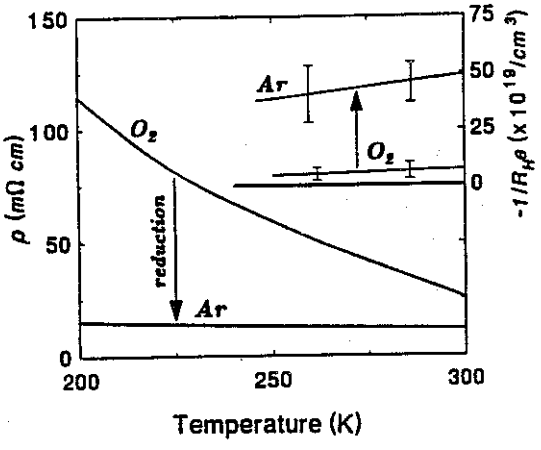

Fig. 3 Effect of reduction on the resistivity and Hall carrier density $1/R_H e$ for a $Sr_xCuO_{2-\delta}$ film grown by atomic layer deposition. Note the negative sign of the Hall carrier density.

to reports for the high-pressure synthesized bulk ceramics [3], the lower resistivities do not result from hole-doping, but rather from *electron-doping*. Remarkably similar resistivities resulted after oxidation in 1.0 atm oxygen. (ii) Hole-doping is enhanced (electron-doping reduced) at higher oxygen pressures (film 4) and lower substrate temperatures (film 5). The correlations for films grown with the laser-MBE technique are similar. With this technique, the epitaxial growth of each unit-cell layer represents a distinct event which may be recorded via the induced variations in the RHEED pattern. Variations in the Sr/Cu stoichiometry can be instantly applied by adjustment of the number of laser pulses admitted to the individual Sr (metal) and CuO (sintered) targets. In this way, the deposition (composition) may be adjusted to optimize continuity of a streaky RHEED pattern (indicating a smooth surface with small surface steps) and vigorous intensity oscillations. As described in more detail in [10], post-growth characterization indicates that these periodic, layer-by-layer films exhibit a tendency towards *electron-doping and Sr-deficiency*. The apparent balance between deposited and incorporated species under these controlled growth conditions suggests that these are *natural tendencies for the $SrCuO_2$ infinite layer matrix*. On the other hand, gross deviations in the layer-by-layer deposition scheme or excess Sr(O) deposition systematically lead to hole-doping. Together with the data of Fig. 2, these observations suggest that the hole-doping arises from Sr atoms expelled from the (Sr-deficient) infinite layer matrix, possibly forming extended defects with oxygen atoms in apical coordination towards the CuO_2 sheets.

Hall and thermo-electric power measurements confirm the existence of the distinct doping mechanisms and the tendency towards electron-doping in the Sr-deficient films. The Hall and Seebeck coefficients are dependent on the oxygen content, i.e. the previous low temperature anneal. This dependence is illustrated in Fig. 2 for a layer-by-layer deposited $Sr_xCuO_{2\pm\delta}$ film. It is seen that the resistivity decreases upon reduction of the oxygen content (after annealing in argon) while the absolute value of the "*n*-type" Hall carrier density increases. Taking into account the correlation with the oxygen pressure during epitaxial growth, we assume that the electron-doping in the Sr-deficient films results from oxygen vacancies in the $CuO_{2-\delta}$ sheets, induced to maintain charge neutrality of the overall structure. Conversely, the oxygen vacancies could effect Sr vacancy formation during epitaxial growth. Although relatively low resistivities were obtained, superconductivity was not observed for any of the Sr-deficient films.

Charge neutrality constraints in the growth and oxidation of $Sr_{n+1}Cu_nO_{2n+1}$ films

The first superconducting descendant derived from the $SrCuO_2$ infinite layer films are the Ruddlesheim-Popper phases $Sr_{n+1}Cu_nO_{2n+1}$. These phases are related to the parent structure via the insertion of one extra SrO lattice plane per n unit-cell layers of $SrCuO_2$ [4]. The laser-MBE technique was used to insert these extra lattice planes. Note that the attempt to induce hole-doped superconductivity via the insertion of SrO defect layers follows naturally from the observed carrier doping correlations. The $[SrCuO_2]_n$ infinite layer blocks were co-deposited by laser ablation from a composite $SrCuO_2$ target. The extra SrO monolayers were ablated from metallic Sr. The deposition conditions (NO_2 supply and substrate temperature) were kept the same as for the $SrCuO_2$ infinite layer films.

Distinct spots appeared in the RHEED pattern during the deposition of the extra SrO monolayers. The spots were similar to those observed during layer-by-layer growth upon continued Sr deposition and they indicate that the extra SrO monolayers do not optimally wet the underlying structure, but rather form islands. The spots disappeared only partially during overgrowth with the next $[SrCuO_2]_n$ block ($n = 3$–9). The growth properties could be improved by reducing the NO_2 oxidant supply, however, as discussed previously, the use of mildly oxidizing conditions tends to produce electron-doped properties of the Sr_xCuO_2 matrix. Despite these complications, the extra SrO deposits were effective in inducing hole-doping (as grown) and superconductivity after high-temperature oxygenation. A key parameter for achieving the semiconductor–metal transition depicted in Fig. 1 proved to be the *cooling rate* at the end of the anneals. Conductivity enhancements only occurred upon rapid cooling (performed by sliding the quartz sample holder rapidly out of the furnace hot zone), whereas slower cooling procedures led to an increase of the resistivity [11]. In this context it is important to note that the thin film infinite layer structure becomes unstable at the high annealing temperatures employed. Partial decomposition into the stable insulating oxides Sr_2CuO_3, $Sr_{14}Cu_{24}O_{41}$, and CuO was observed for annealing temperatures $\gtrsim 700$°C. The conductivity enhancements despite this decomposition were observed *only* for films containing the extra SrO deposits. The effect of the cooling rate and the apparently dissimilar behavior for hole-doped and electron-doped films are illustrated in Fig. 4. Note however, that if one takes into account the opposite dependence of the resistivity on the oxygen content for either film, a higher oxygen concentration is indicated by the data in this figure for both films after rapid cooling, suggesting an *oxygen content which increases upon heating.* This behavior is just opposite to that observed for hole-doped superconductors such as $YBa_2Cu_3O_{7-\delta}$.

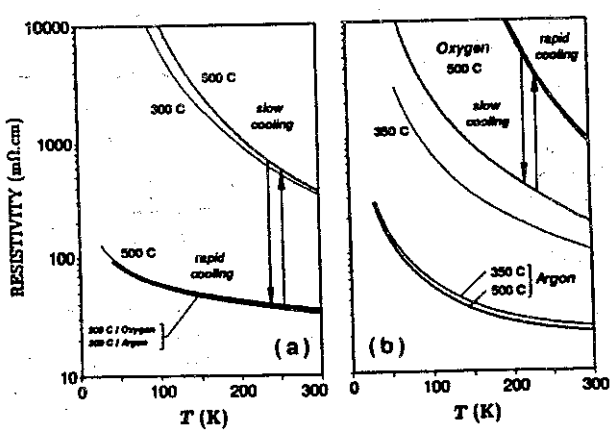

Fig. 4 Effect of cooling rate on the resistivity for (a) hole-doped $Sr_7Cu_6O_{13}$ film containing extra SrO deposits and (b) electron-doped $Sr_xCuO_{2-\delta}$ film grown by atomic layer deposition. The 500°C anneals were performed in the sequence: rapid–slow–rapid (cooling). The anneals at 200°C in (a) were performed after the second rapid cooling anneal at 500°C.

Consideration of the *charge neutrality* constraints associated with the ideal $(SrO)_2$ rocksalt double layers may provide an explanation for this intriguing behavior. Compared to the infinite layer structure, the $(SrO)_2$ double layers in $Sr_{n+1}Cu_nO_{2n+1}$ replace a single layer of Sr^{2+} ions (Fig. 1). Earlier publications by Adachi et al. and Hiroi et al. [4] speculated that the rocksalt layers would contain about 50% oxygen vacancies and that the neighboring CuO_2 sheets would be fully occupied. A recent neutron diffraction study by Shimakawa et al. [18], however, indicates just the opposite, namely that the $(SrO)_2$ layers are fully occupied and that oxygen vacancies are located in the $CuO_{2-\delta}$ sheets. We suggest that a similar oxygen distribution may exist in areas of the film where $(SrO)_2$ double layers are interleaved in the infinite layer lattice, after low temperature oxidation. During the high temperature anneals, additional oxygen could enter the oxygen deficient CuO_2 sheets due to thermal disordering or additional oxygen uptake. Although the "rapid" cooling rate in our study ($\sim$ 50–100°C/min) probably is still slow compared to the oxygen diffusion rate, a partially redistributed oxygen lattice could have been preserved, giving rise to the extra hole-doping and superconductivity. It is interesting that these same charge neutrality constraints also may explain the island-like growth properties of the inserted SrO monolayers: At the high oxidation rates used for stabilization of the infinite layer lattice, the $(SrO)_2$ double layers aimed for would tend to be stoichiometric and thus require large numbers of oxygen vacancies in the topmost CuO_2 sheets. By forming islands, the contact area with the underlying matrix is minimized, and thus the charge neutrality conflict reduced. Although further research is needed to fully establish this correlation, the example of the $Sr_{n+1}Cu_nO_{2n+1}$ films illustrates the unique information that may be deduced from monitoring of the layer-by-layer process.

Structure of $Sr_2CuO_2(CO_3)$ oxycarbonate films converted from $SrCuO_2$

A characteristic feature of the oxycarbonates as well as other oxyanion cuprates are the short metalloid–oxygen bondlengths, similar to those of the corresponding radicals CO_3^{2-}, BO_3^{3-}, NO_3^-, etc. [13]. Thus, the two-dimensional nature of the CuO_2 sheets remains unaffected, as well as the layered chemistry of the HTS cuprates. The structure of the prototype oxycarbonate $Sr_2CuO_2(CO_3)$ has been described by Miyazaki et al. [12]. The CO_3 groups are incorporated in slabs parallel to the CuO_2 sheets, from which they are separated via layers of Sr (Fig. 1). An alternative view is the stacking of alternating layers of $SrCuO_2$ and $SrCO_3$ perovskite-like blocks along a common *c*-axis.

The structure identified for the $SrCuO_2$ infinite layer films after CO_2 conversion is closely related to that described by Miyazaki et al. A θ–2θ x-ray diffraction pattern in the symmetric Bragg reflection geometry for a 300-Å thick film annealed at 700°C in flowing laboratory air (containing 400 ppm CO_2) is shown in Fig. 4. The periodicity calculated from the five newly appeared peaks is 7.49 Å, which agrees well with the stacking periodicity of the two types of perovskite-like blocks. Using off-axis x-ray scans with the four-circle goniometer it was observed that the true unit cell is doubled along each of the three principle axes. Accordingly, the total *c*-axis length is 14.98 Å. A similar superstructure has been

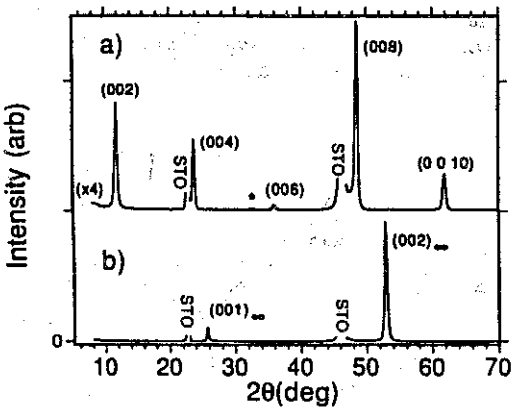

Fig. 5 θ–2θ x-ray diffraction patterns ($CuK\alpha_1$) showing CO_2 induced conversion of $SrCuO_2$ epitaxial film: (a) oxycarbonate phase; indices based on full unit cell with $c = 14.98$ Å. (b) parent lattice.

reported for the stoichiometric bulk compound and has been attributed to a rotational ordering of the flat CO_3 groups. This close structural similarity suggests that the oxycarbonate phase has formed via the substitution of CO_3 for Cu atoms of every other CuO_2 sheet. Indeed, the presence of carbon atoms on substitutional lattice sites was confirmed by ion beam analysis using a sensitive proton backscattering technique [15].

Superconductivity has been reported for the bulk compound after partial substitution of Cu atoms in the CO_3 slabs, facilitated by the simultaneous substitution of Sr with Ba [19]. In the converted films, a mixed (C, Cu) site occupancy could have resulted from the relatively low processing temperatures, leading to a partial retention of Cu atoms in the newly formed CO_3 layers. The hole-doping presumably results from excess oxygen in these mixed (C, Cu) layers. A more appropriate structure formula for the superconducting phase in these films, therefore, is $Sr_2Cu_{1+y}O_{2+2y+z}(CO_3)_{1-y}$, where z denotes the excess oxygen. As shown in Fig. 1, the CO_3 substitution clearly enhanced the carrier density of the semiconductive parent. The $Sr(C, Cu)O_{3-\delta}$ block, therefore, should be considered a new type of charge reservoir for the HTS cuprates.

Concluding remarks

Two superconducting descendants have been successfully synthesized from epitaxial films of the parent compound $SrCuO_2$ by the processing-controlled insertion of charge reservoir layers. The descendants may be considered "first-in-line" because the charge reservoir layers are based on amplification of the role of naturally occurring defects in the infinite layer structure, i.e. locally intergrown SrO defects and isolated CO_3 radicals in the CuO_2 sheets. Although T_c is low compared to previously established HTS cuprates, the first realization of these phases should provide valuable clues for the synthesis of "next-generation" superconductors in epitaxial films.

Research sponsored by the Laboratory Directed Research and Development Program of the Oak Ridge National Laboratory, managed for the U.S. Department of Energy by martin Marietta Energy Systems, Inc. under contract No. DE-AC05-84OR21400.

References

1. T. Siegrist et al., *Nature* **324**, 231 (1988).
2. D. Vaknin et al., *Phys. Rev. B* **39**, 9122 (1989).
3. M. Takano et al., *Physica C* **176**, 441 (1991); M. Azuma et al., *Nature* **356**, 775 (1992).
4. S. Adachi et al., *Physica C* **212**, 164 (1993); Z. Hiroi et al., *Nature* **364**, 315 (1993).
5. M. A. Alario-Franco et al., *Physica C* **222**, 52 (1994); X.-J. Wu et al., *Physica C* **223**, 243 (1994); H. Ihara et al., *Japan. J. Appl. Phys.* **33**, L503 (1994).
6. H. Yamauchi et al., *Japan. J. Appl. Phys.* **34**, L349 (1995).
7. X. Li et al., *Japan J. Appl. Phys.* **31**, L934 (1992).
8. D. P. Norton et al., *Physica C* **217**, 146 (1993).
9. X. Li et al., *Japan. J. Appl. Phys.* **33**, L18 (1994); D. P. Norton et al., *Science* **265**, 2074 (1994).
10. R. Feenstra et al., *Physica C* **224**, 300 (1994).
11. R. Feenstra et al., *Appl. Phys. Lett.* **66**, 2283 (1995).
12. Y. Miyazaki et al., *Physica C* **191**, 434 (1992).
13. C. Greaves et al., *Physica C* **235–240**, 158 (1994); T. Kawashima et al., ibid. **224**, 69 (1994).
14. T. B. Lindemer et al., *Physica C* **167**, 312 (1990); M. Maciejewski et al., ibid. **227**, 343 (1994).
15. R. Feenstra et al., *Appl. Phys. Lett.* submitted.
16. D. P. Norton et al., *Appl. Phys. Lett.* **62**, 1679 (1993).
17. X. Li et al., *Japan J. Appl. Phys.* **31**, L217 (1992).
18. Y. Shimakawa et al., *Physica C* **228**, 73 (1994).
19. K. Kinoshita et al., *Nature* **357**, 313 (1992); F. Izumi et al., *Physica C* **196**, 227 (1992).